
CHAPTER 9

Classification Scheme Using Modified Photometric Stereo and 2D Spectra Comparison

9.1. Introduction

In *Chapter 8*, even we combine more feature spaces and more feature generators, we note that the classification results are not quite as high as those published for some image rotation invariant schemes [Cohen91] [Reed93] [Hayley96] [Port97] [Fountain98] [Zhang02a] [Varma02], as they are good considering the difficulties involved in rotation of real surface textures and the large number of different texture classes presented. In order to justify the cost and problems caused by photometric stereo imaging, such as shadow presented on textures, we present a modified photometric stereo strategy using more images.

Furthermore, one reason of misclassification is that the classification algorithm stops too soon. We only compare *1D* spectra features (*polar* and *radial*) so far, these *1D* spectra are integrals of the original *2D* spectra (*gradient* or *albedo*). Two textures with different *2D* spectra may well have the same *1D* spectra. Therefore a final verification step should be included where the *2D* spectra are compared. This *2D* comparison would not be costly because the rotation angles are already known from their *1D* polar spectra. We finally present the classification scheme using *2D* spectra together with the classification results.

9.2. Photometric Stereo Using More Images

9.2.1. Introduction

All the classifiers presented in this thesis use data obtained from photometric stereo. Their performance therefore depends on the accuracy with which the surface properties are obtained. The method is prone to difficulty sometimes where the parts of the surface are shadowed.

In this section, we will propose an additional strategy for the photometric stereo technique by using more images to estimate surface properties, including both gradient data and albedo data, where we take into account of the effect of shadow. The main advantage of the new method is that surface properties can be estimated more accurately. More images are obtained using further illumination sources, such that more information can be obtained. The improved experimental results obtained from this new strategy are also presented, while comparing to those from our existing simple three image-based photometric stereo strategy, denoted by *PS3*.

9.2.2. The Problem of Shadows in PS3

So far, we have assumed that there are no shadows in the images. But it is clear from our database that this is a poor assumption. In this section, we will show that how much shadows affect our classification scheme.

In the circumstance that we have no control in capturing images of real textures with regard to its physical surface and illumination, we have to simulate a surface both with and without shadow on synthetic textures only. Therefore we only test the performance of the classification scheme in simulated experiments. *Figure 9. 1* shows the classification results for four synthetic textures (*rock, sand, malv and ogil*) for different slant angle σ settings, in terms of those without shadow and with

simulated shadow. We note that while increasing the slant angle of σ , the classification accuracy for the textures with shadow decreases from 100% to 95.83%. On the other hand, whatever the slant angle σ is, the classification accuracy for the textures without the effect of shadow is constant at 100%.

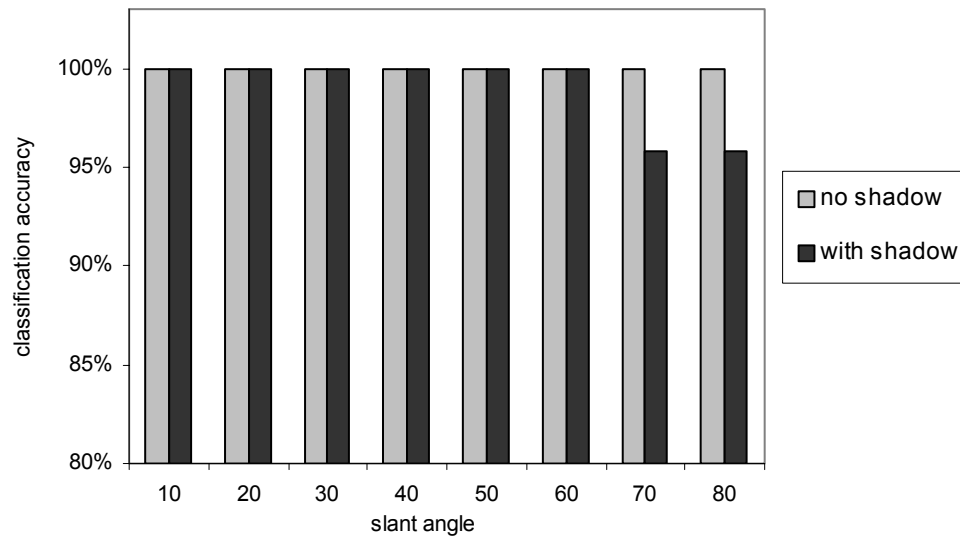


Figure 9. 1 Classification results for four synthetic textures for different slant angle σ settings, in terms of those without shadow and with simulated shadow.

Moreover, it is interesting to see that all of the misclassification only occurred on the directional texture of “sand”. Figure 9. 2 displays images of the texture “sand” with a constant illumination tilt angle of $\tau=0^\circ$ as indicated by black arrows in white circles, while the slant angle is varied ($\sigma=30^\circ$, $\sigma=50^\circ$ and $\sigma=70^\circ$ respectively), and the texture is simulated with and without shadow. We may see the texture of “sand” with shadow results in very unnatural looking images as they have bright spots and dark regions which indicate the effect of shadow.

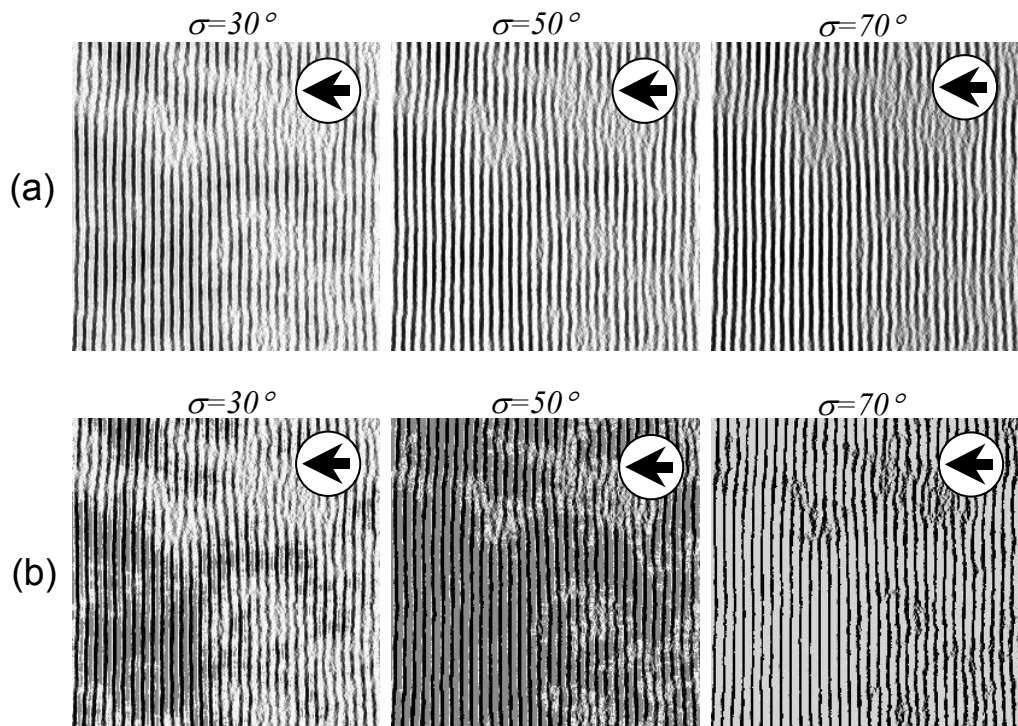


Figure 9. 2 Images of the texture “sand” with a constant illumination tilt angle of $\tau=0^\circ$ as indicated by black arrows in white circles, with the slant angles of $\sigma=30^\circ$, $\sigma=50^\circ$ and $\sigma=70^\circ$ respectively. (a). simulated textures without shadow. (b). simulated textures with shadow.

Things are clearer in the Figure 9. 3, where shadow count against slant angle σ for “sand” with simulated shadow effect is shown. The shadow area is becoming bigger and bigger as the slant angle σ increases. It is the dominant effect of shadow that makes our classifier using photometric stereo fail. In other words, a photometric stereo image set (three images) contains quite a lot of pixels with shadow information which also violates to the assumptions of our simple photometric stereo algorithm (PS3) based on three input images. This motivates us to improve our existing photometric stereo technique in order to remove or reduce the effect of shadows and achieve better performance in the latter stage of classification.

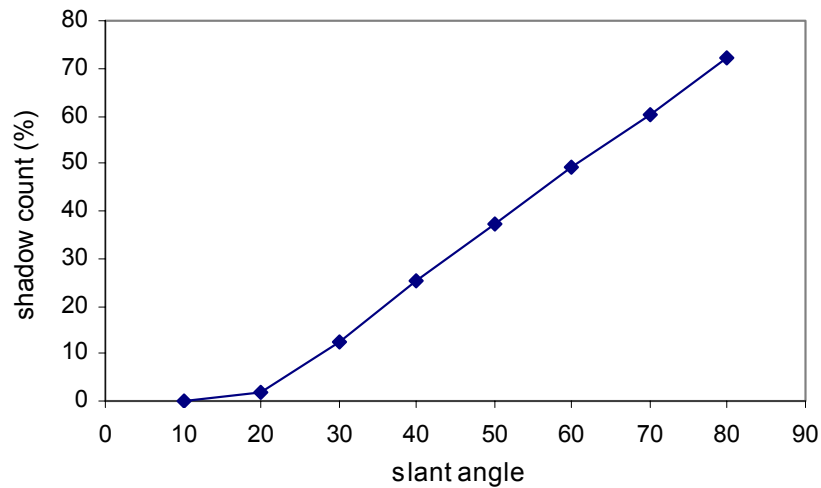


Figure 9. 3 Shadow count against slant angle for texture of “sand” with simulated shadow effect.

9.2.3. Existing Photometric Stereo Techniques (PS3) Obtained from Different Light Sets

So far our current photometric stereo technique (*PS3*) is based on three images taken under the illumination conditions with a constant slant angle σ , with the tile angles of $\tau=0^\circ$, $\tau=90^\circ$ and $\tau=180^\circ$. We may extend this photometric stereo image set into different versions which use different combinations of three input images taken from different illumination directions. *Figure 9. 4* illustrates four different sets of photometric stereo images; each of them has three input images which come from three different illumination conditions with tilt angles of $\tau=0^\circ$, $\tau=90^\circ$, $\tau=180^\circ$ and $\tau=270^\circ$ (as indicated by black arrows in white circles), while the slant angle σ is constant.

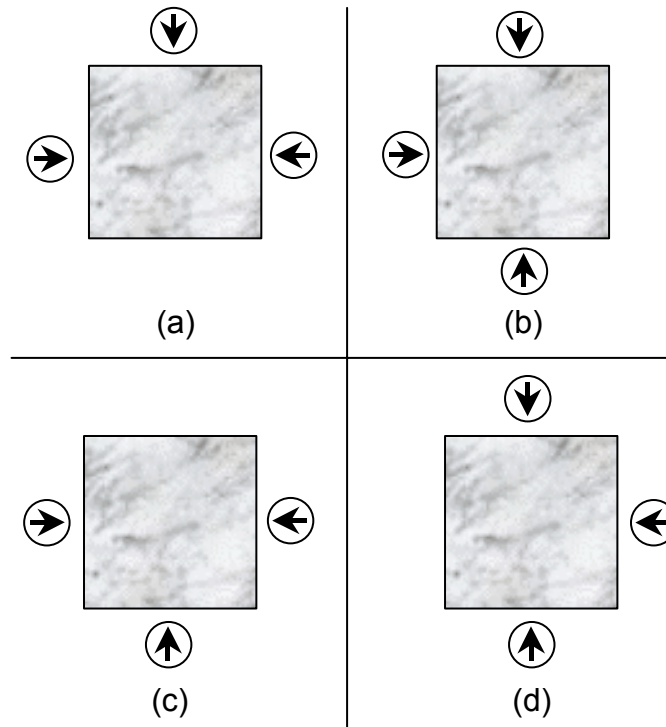


Figure 9. 4 Illustration of four different sets of images, each of them has three input images which come from three different illumination conditions with tilt angels of $\tau=0^\circ$, $\tau=90^\circ$, $\tau=180^\circ$ and $\tau=270^\circ$ (as indicated by black arrows in white circles), while the slant angle σ is constant.

It is interesting to generate the corresponding polar spectra in order to see how robust our features are. For example, Figure 9. 5 shows the polar spectra $\Pi_\alpha(\theta)$ for the texture “sand” with simulated shadow, obtained from the four different sets of photometric stereo images shown in Figure 9. 4. The three input images come from combinations of the illumination conditions as follows:

- a) $\tau=0^\circ$, 90° and 180° (PS3a);
- b) $\tau=90^\circ$, 180° and 270° (PS3b);
- c) $\tau=180^\circ$, 270° and 0° (PS3c); and
- d) $\tau=270^\circ$, 0° and 90° (PS3d).

Each polar spectrum contains those surfaces with different orientation angles of $\varphi=0^\circ$, 30° , 60° , 90° , 120° and 150° .

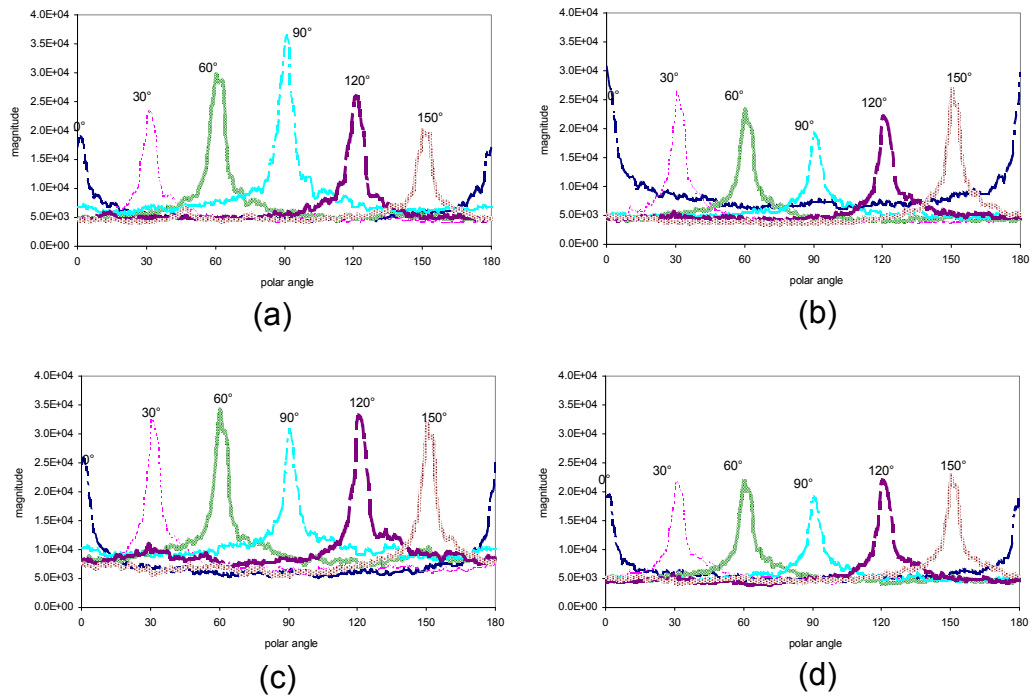


Figure 9.5 Polar spectra $\Pi_{\alpha}(\theta)$ for the texture “sand” with simulated shadow, obtained from four different sets of photometric stereo images. While their respective three input images come from the illumination conditions of (a). $\tau=0^{\circ}, 90^{\circ}$ and 180° ; (b). $\tau=90^{\circ}, 180^{\circ}$ and 270° ; (c). $\tau=180^{\circ}, 270^{\circ}$ and 0° ; (d). $\tau=270^{\circ}, 0^{\circ}$ and 90° . (each polar spectrum contains those surfaces with different orientation angles of $\varphi=0^{\circ}, 30^{\circ}, 60^{\circ}, 90^{\circ}, 120^{\circ}$ and 150°)

It is obvious that the polar spectra vary with the selection of photometric stereo algorithm versions (*PS3a*, *PS3b*, *PS3c* and *PS3d*). In addition, for each algorithm version, the individual polar spectrum corresponding to the surface orientation is not robust to surface rotations. For example, we may see that the magnitude of the peak in the polar spectrum at the same surface orientation such as $\varphi=90^{\circ}$ is either accentuated or attenuated in the different versions of “PS3”. On the other hand, for one version of “PS3”, all of the magnitudes of the peaks at different surface orientations are at different levels due to the artefacts of surface rotation and the effect of shadow.

9.2.4. A New Strategy of Photometric Stereo by Using Four Light Sources (PS4)

As discussed before, we note that the more images we use in photometric stereo, the more information we obtain about the surface. In our new strategy of photometric stereo, we approach the problem of detecting and removing the effect of shadow for the estimation of surface properties by acquiring a set of images of the same surface illuminated from different at least four different directions. Our strategy is to treat the shadows as outliers which can be removed.

- ***Method to remove shadow and specular component***

There are two well-known problems with traditional photometric stereo:

1. There will be some points that will be in *shadow* for one or more of the images; That is, there will not always be three non-zero values to use in solving photometric equation;
2. Surfaces are not truly Lambertian and can have a *specular* component. That is, the reflectance model may be a very bad one for the reflected radiance.

The computer vision literature has many approaches to deal with aspects of these problems (e.g. [Tagare91]). Rushmeier *et al.* [Rushmeier97] present a photometric stereo system to remove the shadow and specular component, using five light sources. In their system, all pixel values with low intensity values must be eliminated from the photometric stereo calculation, and more than three images will be required as inputs. On the other hand, by excluding very high pixel values in the input images, specular effects can be eliminated from the calculation too. Taking into account the above factors, a system is designed to use five light positions that gives five image values from which the high and low values can be discarded and the surface normal can be calculated from the remaining three values.

Drbohalv *et al.* [Drbohalv98] [Drbohalv02] also present a method for detecting shadows and specularities by acquiring a set of images of a scene illuminated from different directions. The method exploits the basic properties of Lambertian surfaces and treats shadows and specularities as outliers. They also note that when there exist

three images in which the brightness value of a given pixel behaves Lambertian, it is enough to predict the brightness of this pixel in *any* image taken under *arbitrary* illumination. In their method, they firstly detect and remove both shadows and specularities and replace their brightness by values corresponding to the Lambertian model of reflectance.

- ***Our PS4 method***

With respect to the textures in our database and system design, we do not consider the specular component. In this section, we therefore propose a PS4 method (photometric stereo method using four light sources) to remove the effect of shadows. It is a simplified Rushmeier's method [Rushmeier97].

Our model from surface to image formation employs the Lambertian model of the surface reflectance, which we assume to be valid with the exception of points in shadow. In other words, we consider only the brightness values of pixels which are not shadowed. While shadow results outliers with respect to the Lambertian model, it also conveys no information about reflectance properties. In a shadowed region, the reflectance information is lost.

When an image of the surface illuminated from a certain direction contains a shadowed region, the necessary way to estimate surface reflectance properties for that specific region is to get another image illuminated by one of four different light sources as shown in *Figure 9. 6*. By increasing the number of images of a surface illuminated from different lighting directions, we will increase the chance that each pixel in the image plane behaves according to the Lambertian model in three of the images.

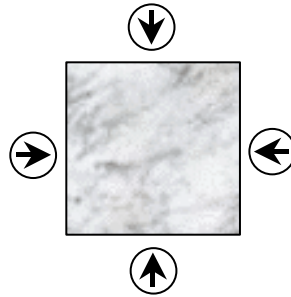


Figure 9. 6 Illustration of a new photometric stereo image set based on four input images (PS4), which comes from four different illumination conditions with tilt angles of $\tau=0^\circ$, $\tau=90^\circ$, $\tau=180^\circ$ and $\tau=270^\circ$ (as indicated by black arrows in white circles), while the slant angle σ is constant.

The scheme of this new algorithm of photometric stereo may take the following form:

```

for each image pixel  $x$  ( $x=0;x<n;x++$ )
{
    select three image pixels  $x_i$ ,  $x_j$  and  $x_k$  among four input image
    pixels  $i_1$ ,  $i_2$ ,  $i_3$  and  $i_4$ ;
    {
        where  $x_i$ ,  $x_j$  and  $x_k$  are the three brightest pixels.
    }
    do
    {
        estimating surface derivatives and albedo using selected three
        pixels of  $x_i$ ,  $x_j$  and  $x_k$  from a selective photometric stereo set with
        three images of  $I_i$ ,  $I_j$  and  $I_k$ ;
    }
}
end

```

To achieve this, we

- 1) first need to able to distinguish pixel with the most shadow from the pixels in each of the four input images based on a pixel by pixel basis. In this case, the darkest pixel is considered to be a shadowed one and the brightest three pixels are used as a set of photometric stereo data for that specific pixel location. In other words, we assume that the outlier pixel is a shadowed one.

- 2) and secondly we have to resolve the surface properties at the corresponding pixel. Shadowed pixels in each set of photometric stereo images can be highlighted in this process with the hope that there are still enough image pixels which are not in shadow. So that we can exclude the shadowed pixel from consideration and recover the surface partial derivatives and albedo using the other three pixels.

The problem of discriminating between less-shadowed pixels and the most-shadowed pixels is crucial. Obviously, if we use less images to estimate the surface properties, the resulting surface properties may be far away from reality. Therefore we use at least four images taken from four different illumination directions to estimate surface partial derivatives and albedo.

In general, our solution to the confounding problems of shadow is to derive images which are shadow free or with minimal shadow: that is to process images such that the shadows are removed whilst retaining all other salient information within the image. Therefore we need a sequence of images, captured with a stationary camera over a period of time, such that the illumination in the scene changes considerably, specifically the position of the shadows.

9.2.5. Improved Experimental Results

In this section we test some of the following aspects by using our improved photometric stereo technique “*PS4*”. Some successful and improved results obtained on “*PS4*” are also presented and compared against those on “*PS3*”.

- ***Detecting shadow area***

At the same time when we estimate surface partial derivatives and albedo data by using the improved photometric stereo algorithm “*PS4*” which uses four images taken under four different illumination directions, we may also detect the shadowed area in the image plane and produce a shadow image. *Figure 9. 7* shows a

successfully detected shadow image for one of the real texture “*rkb1*” which is in our photometric texture database produced by “*PS4*” (the white area indicates the shadows integrated from all four input images). We note that this all-in-one shadow image is valid for all of four input images wherever the illumination direction comes from (tilt angle of $\tau=0^\circ$, $\tau=90^\circ$, $\tau=180^\circ$ and $\tau=270^\circ$).

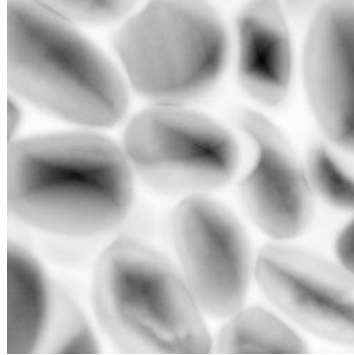


Figure 9. 7 Detected shadow image for real texture “*rkb1*” using four photometric stereo images “*PS4*” (the white area indicates the shadow regions integrated from all four input images).

- ***Estimation of surface relief and albedo image***

The pair of images shown in *Figure 9. 8* are recovered surface relief images obtained using “*PS3*” and “*PS4*” for the real texture “*rkb1*”. Their corresponding recovered surface albedo images are presented in *Figure 9. 9*. We may note that the resulting image obtained using “*PS4*” is better than that obtained using “*PS3*” and provides more detailed information about either the surface relief or albedo. There are some obvious improvements in the images of “*PS4*”. For example, looking at the region *B1*, a better recovered surface relief is apparent in the image for “*PS4*”, and clarifies the darker region in the image for “*PS3*” which is due to the effect of shadow. With regard to the albedo image, the region *B2* obtained using “*PS4*” reveals more correct albedo information than that obtained using “*PS3*”.

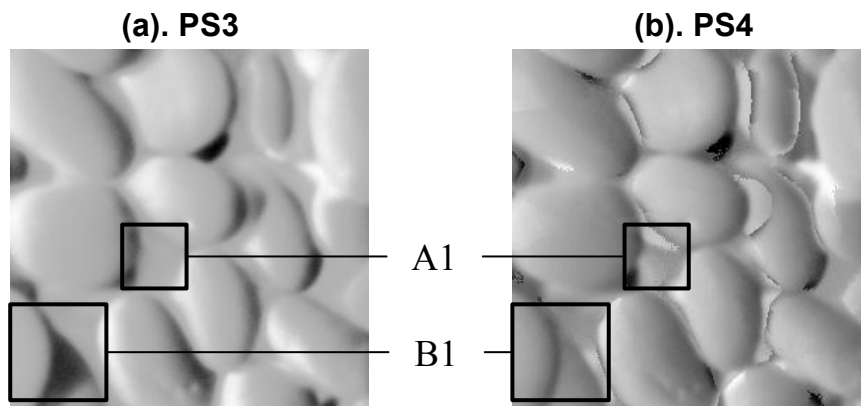


Figure 9. 8 Recovered surface relief images obtained from “PS3” and “PS4” for real texture “rkb1”.

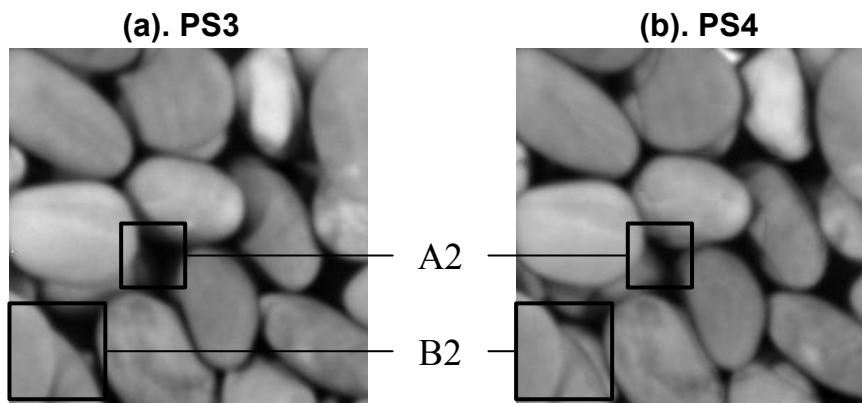


Figure 9. 9 Recovered surface albedo images obtained from “PS3” and “PS4” for real texture “rkb1”.

- ***Polar spectra to be robust to surface rotation***

Figure 9. 10 shows the polar spectrum $\Pi_{\alpha}(\theta)$ of gradient spectra $M(\omega, \theta)$ for the synthetic texture “sand” with simulated shadow at surface rotations of $\varphi = 0^{\circ}, 30^{\circ}, 60^{\circ}, 90^{\circ}, 120^{\circ}$ and 150° , which are obtained using “PS4”. We may note that the magnitude and shape of these polar spectra, whatever the surface orientations are, are robust to surface rotation, compared to those results obtained from “PS3” shown in Figure 9. 5.

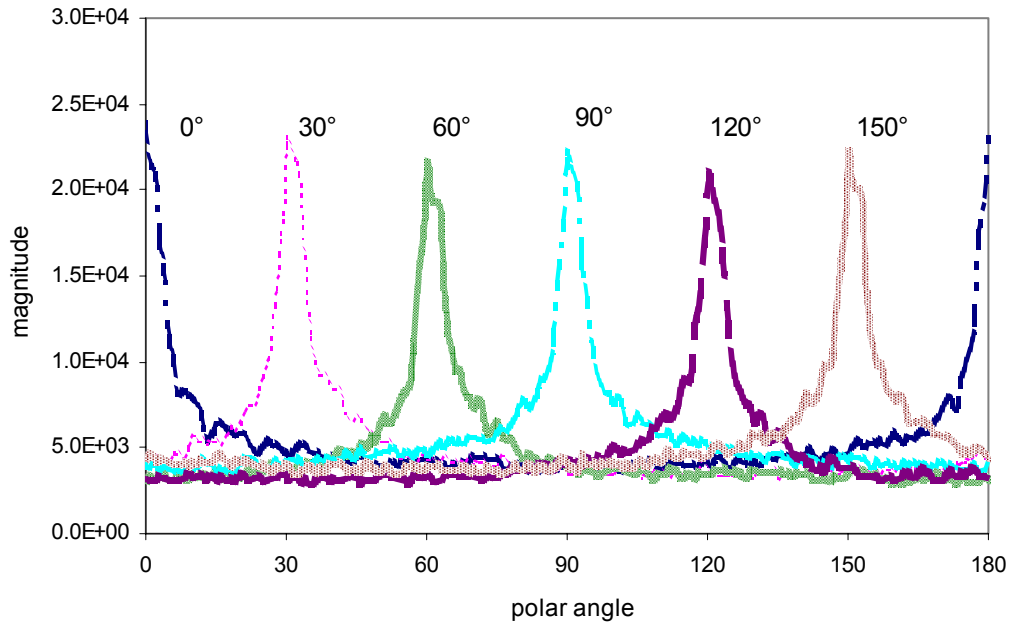


Figure 9.10 Polar spectra $\Pi_{\alpha}(\theta)$ of gradient spectra $M(\omega, \theta)$ for synthetic texture “sand” with simulated shadow at surface rotations of $\varphi = 0^{\circ}, 30^{\circ}, 60^{\circ}, 90^{\circ}, 120^{\circ}$ and 150° , which are obtained by using “PS4” ($\tau=0^{\circ}, 90^{\circ}, 180^{\circ}$ and 270°).

In general, the technique of “PS4” presented in this section is better than “PS3” by using one more input photometric stereo image, and we will incorporate it into our new improved surface rotation invariant classification scheme which is summarised in next section.

- **Classification results (PS3 vs. PS4)**

Figure 9.11 shows the classification results for 30 real textures between PS3 and PS4 method. A classification accuracy of 90.56% (Section 8.4.2) is achieved by PS3 method. On the other hand, a classification accuracy of 95.93% is achieved by PS4 method, where the shadow artefacts are removed by introducing one more image for each photometric stereo data set. In general, PS4 method has better performance than PS3. More images, more information about surfaces.

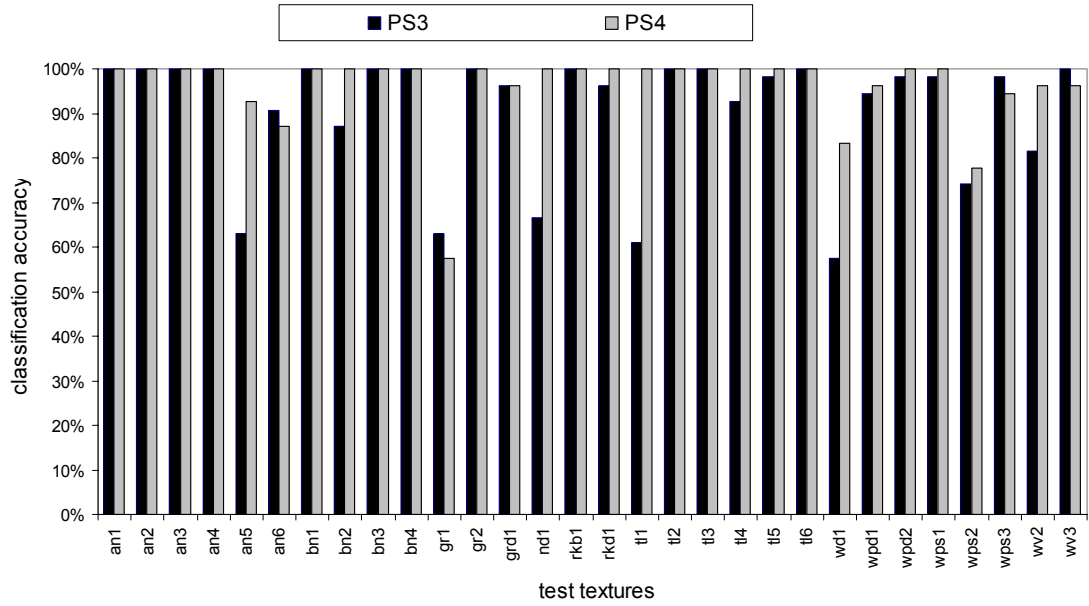


Figure 9.11 Classification results for 30 real textures between PS3 and PS4 .

9.3. Classification Scheme Using 2D Spectra Comparison

Comparing to the classification algorithms based on polar and radial spectra of 2D gradient spectra M and albedo spectra A , which are presented in Chapter 6, 7 and 8, we propose a new classification scheme directly using 2D spectra themselves.

After investigation of image-based classifier against surface-based classifier in Chapter 6, 7 and 8, we note that for 3D surface rotation invariant texture classification, we have to use surface information obtained by photometric stereo instead of only using image information in order to make the classification scheme robust to surface rotation.

9.3.1. Classification Scheme

As discussed before, one reason of misclassification presented previous chapters is that the classification algorithm stops too soon. We only compare 1D spectra features

(polar and radial) so far, these 1D spectra are integrals of the original 2D spectra (gradient or albedo). Two textures with different 2D spectra may well have the same 1D spectra. Therefore a final verification step should be included where the 2D spectra are compared. This 2D comparison would not be costly because the rotation angles are already known from their 1D polar spectra. Figure 9. 12 presents the classification scheme using modified photometric stereo (PS4) and together with 2D spectra comparison.

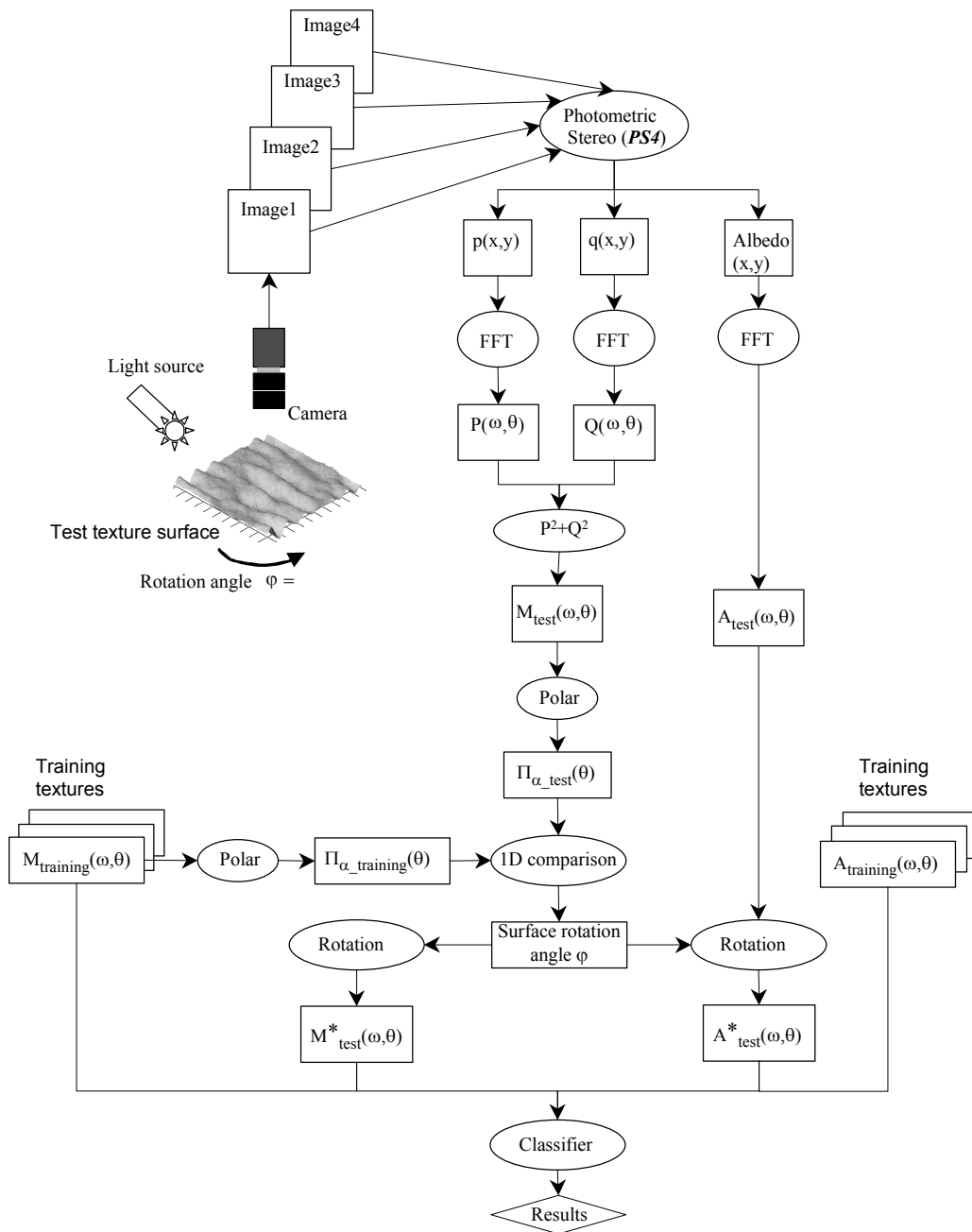


Figure 9. 12 Surface rotation invariant texture classification scheme using modified photometric stereo (PS4) and 2D spectra comparison.

The classification scheme can be summarised as follows:

1. Surface gradient spectra $M_{test}(\omega, \theta)$ and albedo spectra $A_{test}(\omega, \theta)$ of test textures can be estimated using modified photometric stereo (PS4, discussed in last section), where each photometric stereo image set contains four images taken at illuminant tilt angles (τ) of 0° , 90° , 180° and 270° respectively.
2. 2D Gradient spectra $M_{test}(\omega, \theta)$ of test textures are processed to provide 1D polar spectra $\Pi_{\alpha_{test}}(\theta)$. In the same way, 2D gradient spectra $M_{training}(\omega, \theta)$ of training textures are processed to provide 1D polar spectra $\Pi_{\alpha_{training}}(\theta)$.
3. The 1D polar spectrum $\Pi_{\alpha_{test}}(\theta)$ of test texture is then compared with the 1D polar spectra $\Pi_{\alpha_{training}}(\theta)$ obtained from training textures in order to estimate surface orientation angle φ . This step can be done by calculating SSD values presented in section 6.4.6.
4. The 2D Gradient spectrum $M_{test}(\omega, \theta)$ of test texture is therefore rotated by estimated surface orientation angle φ to provide the 2D rotated gradient spectra version $M^*_{test}(\omega, \theta)$. At the same time, the 2D albedo spectrum $A_{test}(\omega, \theta)$ of test texture is also rotated by angle φ to provide the 2D rotated albedo spectra version $A^*_{test}(\omega, \theta)$. This step results in that both the 2D gradient spectra and 2D albedo spectra between test and training textures have the same surface orientations.
5. The total sum of squared errors statistic is calculated by 2D spectra comparison and the lowest score provides the classification decision.

9.3.2. Classification Results

Figure 9. 13 shows the classification results per texture for two versions of the classifiers using 2D spectra comparison and 1D spectra comparison. The classification accuracy of 95.93% (based on PS4 method, referred Section 9.2.5) is achieved by using 1D spectra only. A better performance with classification accuracy

of 99.07% is improved by comparison of 2D spectra. Note that both classifiers use PS4 photometric stereo method. In general, considering the fact of that we perform the classification on real surface rotation rather than synthetic surface rotation, our classification accuracy does not reach 100%. On the other hand, we ignore the specular-reflection and inter-reflection in fact existing on the real surfaces, which result in misclassification occurred.

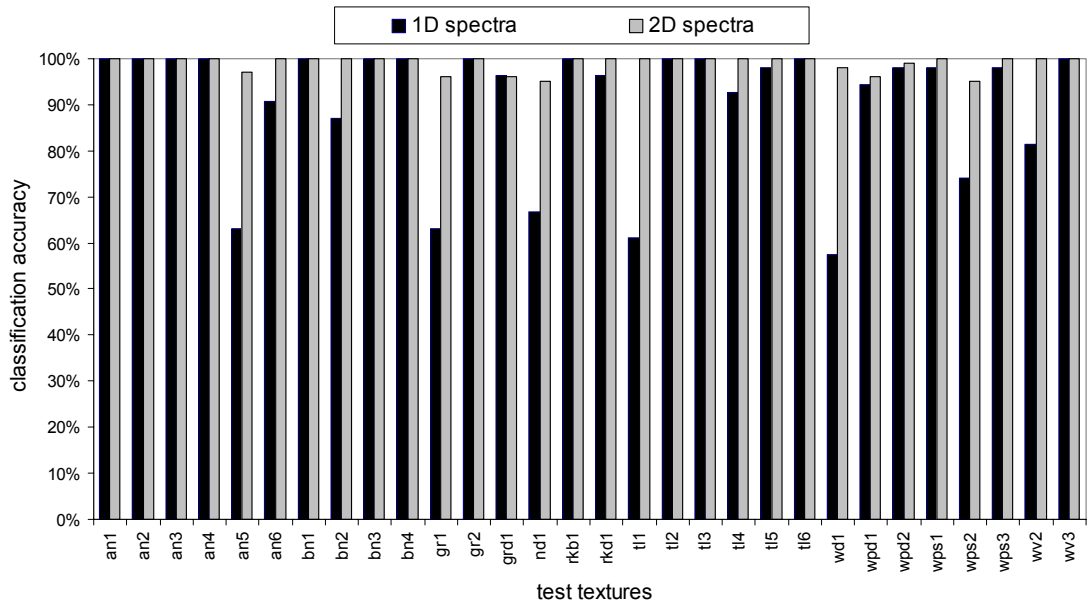


Figure 9. 13 Classification results for 30 real textures between 2D spectra comparison classifier and 2D spectra comparison classifier. (Note that both of them use PS4 photometric stereo method).

We note that the classification scheme presented in Figure 9. 12 is successful and achieves the best classification results for our real texture database. The results also shows that the combination of 1D spectra and 2D spectra makes the classifier to be robust to surface rotation. Furthermore, the estimated surface orientations calculated from 1D polar spectra keep the classification scheme in less computation, since we don't have to perform the heavy-computational 2D image rotation of gradient spectra in very possible orientation angle of test surface texture in order to match with 2D gradient spectra of training textures.

9.3.3. Comparing with Varma and Zisserman’s Method

Table 9. 1 summarises the comparative studies between our method (PS4) and Varma and Zisserman’s Method.

	Our Method (PS4)	Varma and Zisserman’s Methods
Classification Accuracy	<i>99.07%</i>	<i>100%</i>
Number of Classes	<i>30</i>	<i>30</i>
Number of Classifications	<i>1620</i>	<i>840</i>
Number of images per texture class for training	<i>4</i>	<i>28</i>
Number of images per texture class for test	<i>54</i>	<i>28</i>
Computational Cost	<i>Heavy (2D spectrum rotation)</i>	<i>Medium (histogram of texton labelling)</i>
Robustness to surface rotation	<i>Excellent (with surface orientation estimation)</i>	<i>Good (no estimation of surface orientation)</i>
Ease of deployment	<i>Need 4 images / texture for both test and training to estimate feature space</i>	<i>1 image / texture for test, however need 28 images per texture for training</i>
Suitability for applications	<i>Controlled illumination conditions</i>	<i>Unknown illumination directions</i>

Table 9. 1 Comparative study between our method (PS4) and Varma and Zisserman’s method.

9.4. Summary

In this chapter, the problem of shadowing using three-image photometric stereo (*PS3*) is considered. We therefore develop a four-image photometric stereo (*PS4*) to provide more accurate *3D* surface texture properties and to reduce shadow artefacts. With regarding to the classification design, we combine the *1D* spectra and *2D* spectra feature sets to achieve a better classification accuracy of *99.07%*. It uses both *2D* gradient spectra data and *2D* albedo spectra data. In order to make the classifier to be robust to surface rotation, the surface orientation angles are estimated by *1D* polar spectra in the first step. Therefore the classification decision depends on the comparison of *2D* spectra data.